Coverage Path Planning on Multi-depot, Fuel Constraint UAV Missions for Smart Farm Monitoring

Anton Louise P. de Ocampo
Gokongwei College of Engineering
De La Salle University
Manila, Philippines
anton_louise_deocampo@dlsu.edu.ph

Argel A. Bandala
ECE Department
Gokongwei College of Engineering
De La Salle University
Manila, Philippines
argel.bandala@dlsu.edu.ph

Elmer P. Dadios
MEM Department
Gokongwei College of Engineering
De La Salle University
Manila, Philippines
elmer.dadios@dlsu.edu.ph

***Abstract*—UAVs used in monitoring crop fields are flying higher than 6 meters and capture telemetric data that provides information on the general condition of the plants in the field. But, in order to obtain specific information on the actual conditions of the plants based on individual morphological aspects, lower altitude monitoring, at most 3 meters, is required. Low-altitude missions cover less than high-altitude and requires UAVs to fly longer to cover more area. In this paper, an approach for multi-depot, fuel constrained coverage path planning is presented. First, target coverage is segmented into smaller regions based on the number of available charging depots. Then, each region is further decomposed into multitude of cells with area equivalent to the camera FOV when UAV is flying at 3 meters above the field. All possible routes are generated and fed into evolutionary optimization in aim to identify the optimal path considering the fuel constraints and availability of recharging depots. The optimization yields a significant improvement in obtaining the route that will provide the minimum distance that the UAV should traverse to cover the entire Area-of-Interest. This approach proved to be useful for crop field monitoring using UAVs.**

***Index Terms*—Coverage Path Planning, Low-altitude UAV Missions, Genetic Algorithm, Smart Farm Monitoring**

I. Introduction

One of the many applications of Unmanned Aerial Systems is on agriculture in which, these systems are remotely piloted to gather telemetric data of the crop field of interest [1]. The UAVs used for crop field monitoring usually fly at high altitudes to cover larger areas and to complete missions faster. This approach adds flexibility on reconfigurability and relevance of the data type gathered. Sometimes, to monitor condition of plants, captured data from high-altitude drones such as vegetation (NDVI), plant water stress status, crop field temperature [2], [3], [4], plant height field texture [5] and geometric features of trees for forestry monitoring such as canopy area and tree height [6], may not be enough.

In monitoring crop field for the possible presence of plant diseases, one must take a closer investigation on the morphological aspects of the plants. Current methods of plant disease detection can be classified into direct and indirect methods of which the latter includes Thermography, Fluorescence Imaging, Hyper-spectral imaging, and Gas Chromatography to name a few [7]. For automated detection and recognition of plant diseases, images are taken to analyse the effect of the disease to the physiological characteristics of the plants. To obtain relevant information, cameras should be placed at close proximity from the plants. A recent study summarizes the different approaches and methodologies on the use plant images for detection of diseases. All of these methods require that the images must be taken as close as possible from the subject with the highest resolution and minimum image noise [8].

Using UAVs to closely monitor plants, low-altitude flying missions are needed. The problem with low-altitude flying, the drone must travel more to cover as much as that of high-altitude UAVs can cover. Another option to cover more area is to deploy swarm of UAVs which have the capability to recognize each other [9] and can autonomously avoid obstacles[10]. Although using low-altitude UAVs has the advantages of faster deployment, easy reconfiguration, and better wireless communication due to shorter direct wave links, the energy constrains in these low-altitude UAVs limit the extent of its potential in monitoring applications[11]. Coverage Path Planning (CPP) is the term used to define the intended course that UAV or UGV should traverse to cover specific areas of interest. In CPP for UAVs, several challenges arise with respect to identification of shortest path possible [12], creation of a suitable 3D trajectory plan [13] [14], awareness of system's energy capacity [15] [16], and coverage of a much larger area [17], to name some. In some cases, pre-

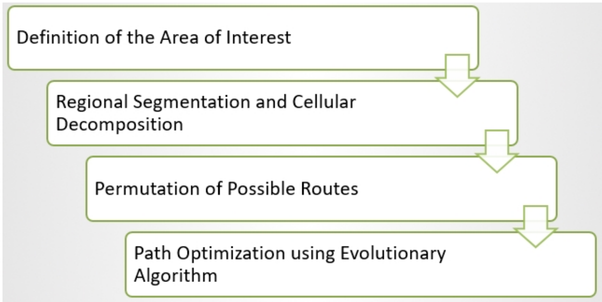

Fig. 1. Methodology for Coverage Path Planning and Optimization.

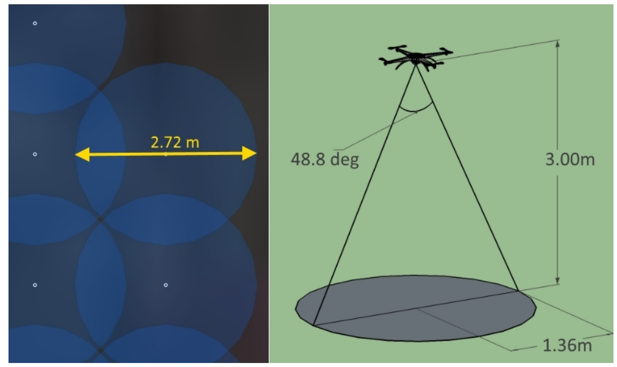

Fig. 2. (Left) The size of the cell covered by the camera FOV at 3m above ground. (Right) Quadrotor directly atop a cell. Quadrotor here is just for visualization and not describes the actual model.

defined path plans are already prepared regardless of the characteristics of the target area. In such systems, the path planner just picks the most suitable path plans from the available sets and perform minor adjustments to suit the mission [18]. To cover larger areas, multiple UAVs can be deployed. These drones are interconnected through Internet-Of-Things which provides faster data transmission and scalability [19].

In agricultural applications, UAVs can be used with UGV for wider coverage and so as not to spend much energy on the UAVs flight [20]. But when using UAV alone in covering a vast agricultural area, Coverage Path Planning that considers fuel constrains of the UAVs is needed to provide full coverage of the target area. In this paper, an algorithm for coverage path planning on a multi-depot, fuel constraint UAV mission for monitoring crop fields is presented. The flight altitude used in this work is just 3 meters above the field and it is assumed that the maximum distance allowed by the capacity the battery for the UAV to traverse is just 700 meters. The remainder of the paper is organized as follows: Section 2 presents the methods performed in the conduct of data gathering, algorithm development and experimentation; Section 3 reports experimental results which validates the proposed approach; and, Section 4 concludes by providing the most relevant results and the summary of the presented work.

II. Methodology

The first task at hand in coverage path planning requires that the Area-of-Interest be defined. To do this, a high-altitude aerial view of the whole target area is captured. The Area-of-Interest is then segmented into regions which are further decomposed into cells. The centres of these cells became the locus or routes that the UAV should traverse. All possible routes are generated by permutation then fed to an evolutionary algorithm for optimization. Then the near-optimal routes are subjected to fuel constraint to identify when the UAV should go back to the depot to recharge. Figure 1 shows the workflow followed in this work.

A. Algorithm for Region Segmentation and Cellular Decomposition

In **Algorithm 1**, the Area-of-Interest is defined. Several depots are arbitrarily deployed with the Area-of-Interest. Then, area is divided into cells. If there still portions of the Area-of-Interest that doesn't belong to any cell, then the cells are overlapped. Then, the distance of certain cell to the depots deployed are calculated. Cells nearest to a certain depot become a single region. The number of regions is based on the number of charging depots. In this research, seven charging depots are arbitrarily position within the target area which is further decomposed into fixed-size cells based on area covered by UAV camera FOV at 3 meters above the crop field. Figure 2 shows the aperture of the camera and the respective Field Of View, FOV, at 3 meters above ground. Regional segmentation is based on the cells' distances from all the depots. The cells nearest to a depot are designated to a similar region.

Algorithm 1 Pseudocode for Region Segmentation

1. A = Defined Area;
2. D = Coordinates of the depots;
3. S = cellular size;
4. **MeasureArea[A]**; *Measure the total area*
5. **while** areaIsNotYetCovered **do**

Decompose[A]; *Decompose area into cells (C) of size (S)*

if U $>$ 0; ***U*** *is uncovered area or not belonging to any cell(C)*

Overlap[C]; *Overlap cells*

end while;

6. **Distance[D to C]**; *Measure distance from depot to every cell*
7. **FindNearestDepot**; *Cells nearest to a depot become a Region*

5. **end**

Algorithm 2 Pseudocode for Genetic Algorithm

1. t = 0;
2. **InitPop**[***P(t)***]; *Generate an initial random routes*
3. **EvalPop**[***P(t)***]; *Calculate the total distance for each route*
4. **while** isNotTerminated **do**

P'(t) ← Variation[***P(t)***]; *Breed new routes (solutions)*

EvalPop[***P'(t)***]; *Evaluate the new routes*

P(t+1) ← ApplyGeneticOperators [*Mutation*];

t ← *t+1*;

5. **end while**

B. Algorithm for Optimization

Genetic Algorithm (GA) has been a well implemented algorithm when it comes to optimization problem because of its robustness and flexibility to be aligned to a very specific problem at hand such as optimization done in [21]. In similar case, GA is used to obtain local path plan for a two-point route [22]. In this paper, GA is used to find the near-optimal route that the UAV can traverse to cover an area-of -interest. Optimization is done per region as to speed up the process. In **Algorithm 2**, **InitPop** generated a random population of 500 routes and evaluated (**EvalPop**) based on distance covered by each route. Based on the evaluated routes, the top 125 fittest routes with the least distance are allowed to mutate to create the next generations. The chromosome model used is a vector of cell centres which represent the waypoints UAV needs to traverse. For each iteration (generation), shown inside the **while** loop, the chromosomes of 2 parents are altered by either flipping, segment swapping, or simply sliding in one some part of a chromosome into the other. Each individual of the current population is evaluated using distance measurements. Upon termination of the process, the most fitted solution or the route with the least distance is annotated as the most optimal solution. For distance measurements, spherical distance is used instead of linear distance due to the fact that the route lies on surface of a sphere. Haversine distance formula as described in Equation (1) is used to evaluate distances between points.

$$d = 2\rho \arcsin(\sqrt{\alpha + \beta}) \tag{1}$$

$$\alpha = \sin^2 \frac{(\varphi_2 - \varphi_1)}{2} \tag{2}$$

$$\beta = \cos(\lambda_1)\cos(\lambda_2)\sin^2(\frac{\lambda_2 - \lambda_1}{2}) \tag{3}$$

In equations (1),(2) and (3), d is the spherical distance between two points in the surface of a sphere, ρ is the spheres radius, φ_1 and φ_2 are the latitudes of points 1 and 2 respectively, in rad, and λ_1 and λ_2 are the longitudes of points 1 and 2 respectively, in rad.

C. Algorithm for Generation of Routes Including the Depots

It must be guaranteed that the UAV can go back when the fuel is near depletion. To do this, the UAV needs to monitor the current fuel level and compute for fuel required to go back to charging depot. In **Algorithm 3**, **R** is the defined route for which the UAV should follow. **Wi** is the waypoint to the next cell. Ideally, UAV would traverse all the waypoints from **Pref** to **Pn** to cover the desired area. However, once the fuel is decreased to a minimum value which is just enough to direct back to the charging depot, the UAV will cancel the next waypoint **Wi+1** and instead follow **Wref**. The centres of the cells within a region are labelled with **P1** to **Pn** while the charging depot is designated as **Pref**. In this study, the term route is defined as the succession of waypoints for the UAV to travel. In succeeding figures, waypoints, labelled as **W1** to **Wn** are the lines connecting two cell centres or points.

Using the best route derived from optimization, the total distance travelled as well as the distance towards the next hop is monitored in addition to the distance from the nearest depot. The capacity of the UAV is decremented after each hop and after each hop, the UAV can still go back to depot for recharge. Figure 3 shows the default route, the next hop and the route towards the depot. **Pref** is the location of the charging depot, while **P1** to **Pn** are the default routes given that the UAV has the capacity to travel all the way from **Pref** to **Pn** back to **Pref** without recharging.

III. Results and Discussion

The crop field where the coverage path plan is mapped is the farm of Mega Nursery Orchids located at 121.11577 longitude, 13.91875 latitude or at Lipa City, Batangas, Philippines. Figure 4 shows the aerial view of the field and Figure 5 shows the arbitrarily chosen locations of the seven charging depots marked by green dots as well as the overlapping cells denoted by blue shades. The area covered by each cell extends only up to 5.81 sq.meters.

Algorithm 3 Pseudocode for Route Generation including Depots

1. ***t***=0; *Initiation*
2. **R** = Defined Route; *Define route to follow*
3. **while** isRouteNotCovered **do**
4. ***Traverse(Wi)***; *travel the ith waypoint*
5. **if** Fuelcurrent > Fuelmin **do**
6. ***Traverse(Wi+1)***;
7. **else do**
8. ***Traverse(Wref)***; *Return to charging depot*
9. ***i* = *i* + *1***
10. **end if end while**

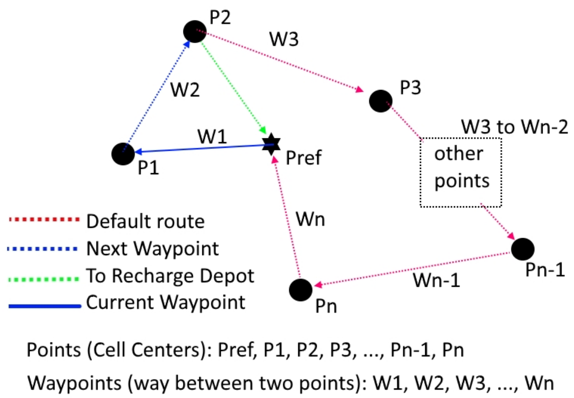

Fig. 3. Routing Options for UAV. Pref is the charging depot and P1 to P2 represent the cells in a certain region

Fig. 4. Aerial View of the Crop Field. Mega Nursery Orchids is located in Lipa City, Batangas, Philippines 4217.

It is important to annotate each region so that the waypoints between regions can be included in the optimization. The result of regional segmentation is shown in Figure 6. The small dots of different colors are markers for cell centres, while green markers denote the location of the charging depots which are then connected by blue lines showing the route that the UAV shall travel when transferring from one region to another. It can be noted that although the depots' coordinates are defined in sequence, the optimization algorithm identified the best route as a closed path passing through points 6,7,5,4,1,3,

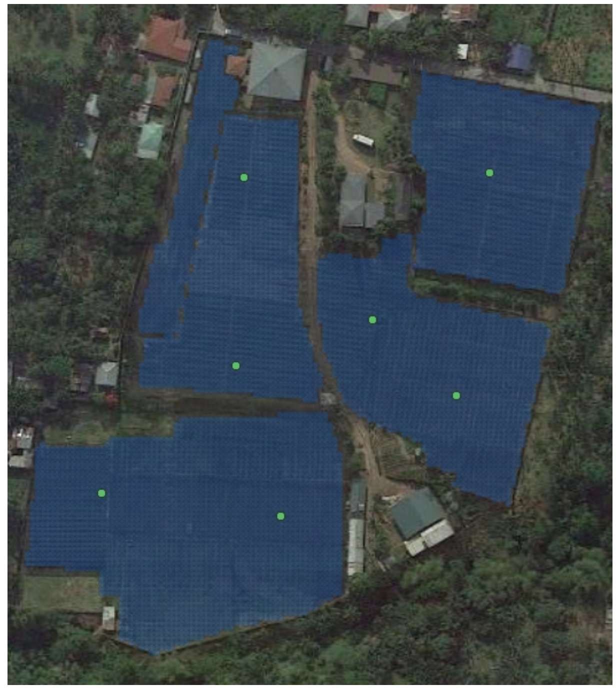

Fig. 5. Charging Depot Placement. The green dots are the locations of the depots. Blue shades are overlapping circles representing the cells.

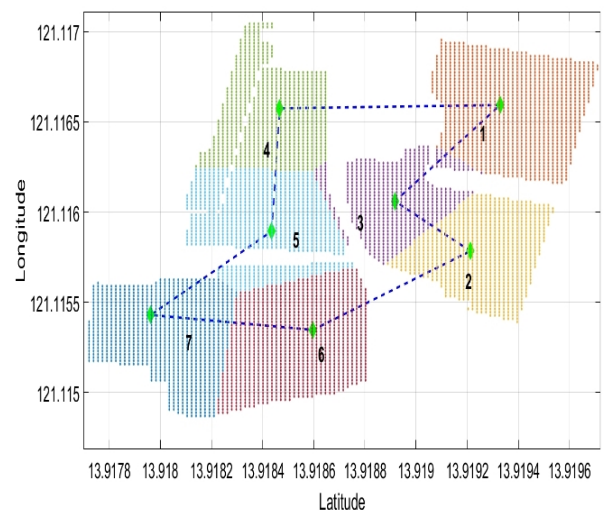

Fig. 6. Regional Segmentation. Colored dots represents the cells in different regions designated by numbers [1-7]. Dash lines represent the route between regions. Green markers are the location of the depots.

and 2. For the optimal route within a certain region, the optimization process evaluates all the possible routes using distance matrices. Figure 7 shows an excerpt from the 662 x 662 distance matrix of region 3. Each column represent the distance of that point to the corresponding point in the rows of the matrix.

Before the UAV transfers from one region to another,

	P1	P2	P3	P4	P5	P6	...	Pn
P1	0	0.004336	0.006132	0.006992	0.007995	0.008672	...	0.071773
P2	0.004336	0	0.001939	0.002742	0.003878	0.004336	...	0.067869
P3	0.006132	0.001939	0	0.001939	0.001939	0.002742	...	0.065929
P4	0.006992	0.002742	0.001939	0	0.002742	0.001939	...	0.065958
P5	0.007995	0.003878	0.001939	0.002742	0	0.001939	...	0.06399
P6	0.008672	0.004336	0.002742	0.001939	0.001939	0	...	0.06402
⋮	⋮	⋮	⋮	⋮	⋮	⋮	.	⋮
Pn	0.071773	0.067869	0.065929	0.065958	0.06399	0.06402	...	0

Fig. 7. Excerpt from the Distance Matrix of Region 3. The actual size of the Distance Matrix is 662 x 662.

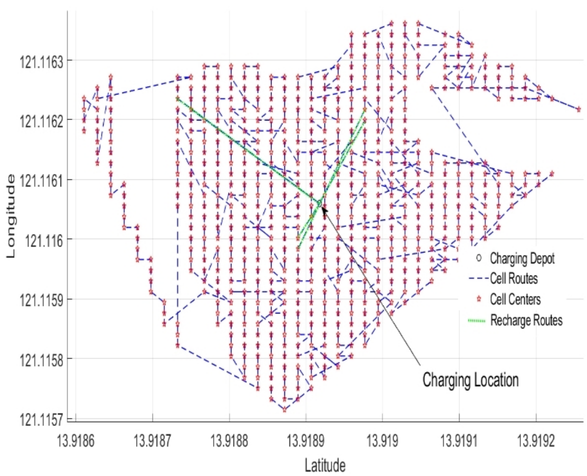

Fig. 8. Optimized Route for Region 3. Green lines show that UAV returns and leave the charging depot at some instances during the scan.

all the cells inside the region under scanning should be covered. There is a total of (n-1)! possible routes that can be used to cover the region of interest, where n is the number of cells in the region, exclusive of the number of times that the UAV will recharge. A sample of the optimized route generated in this work is shown in Figure 8. The red markers are the centres of the cells while the blue line shows the routes to cover the whole region. The green lines are the routes from and toward the depot.

The objective of optimization is find the optimal route that can cover the whole Area-of-Interest with the least distance travelled. Table 1 shows the total distances travelled for each region using the default route, the worst possible route, and the optimized route. The default route

TABLE I
COMPARISON OF ROUTES

Region	Default*	Worst	Optimized	Distance Reduced**
1	62.5604	90.2869	3.5450	94.33
2	37.0341	53.2487	2.3653	93.61
3	28.9933	37.8274	1.7212	94.06
4	34.2466	58.2916	2.3704	93.08
5	46.7383	61.1371	2.6615	94.31
6	44.7843	84.6173	3.3962	92.42
7	44.3966	70.3361	2.9433	93.37
Total	298.75	455.75	19.00	93.64

*Distance traversed is in km.
*Distance reduced is in percent based on the default route.

is a randomly chosen route from all the possible routes within a region which are generated by permuting all the cell centres. The worst route, on the other hand, is taking all the farthest points from one center to another. Significant improvement has been achieved using the optimized route instead of the default route. For example, in Region 1, the decrease in distance from the default route to optimized route is 94.33 percent. In summary, to cover the whole Area-of-Interest using the default route, the UAV needs to travel a total of 298 km distance, while by using the optimized route, the UAV only needs to traverse 19 km which is equivalent to 93.64 percent decrease in total distance.

IV. CONCLUSION

Coverage path planning for a UAV flying at approximately 3 meters from the field becomes cumbersome due to the multitude of cells to be covered. The presented method successfully found the optimal route by considering the fuel capacity as well as the availability of the charging depots. The randomly selected route (default route) has been decreased to an average of 93.64 percent in terms of the distance that the UAV should traverse to fully cover the Area-of-Interest. For future work, heuristic approach combined with evolutionary optimization can be further investigated.

ACKNOWLEDGEMENT

The authors would like to thank DOST-ERDT and the Gokongwei College of Engineering-De La Salle University, for their support on the development of this research work.

REFERENCES

[1] G. Pajares, "Overview and Current Status of Remote Sensing Applications Based on Unmanned Aerial Vehicles," Photogrammetric Engineering and Remote Sensing, vol. 81, no. 4, pp. 281-329, 2015.

[2] F. A. Vega, F. C. Ramrez, M. P. Saiz and F. O. Rosa, ”Multi-temporal imaging using an unmanned aerial vehicle for monitoring a sunflower crop,” Biosystems Engineering, vol. 132, pp. 19-27, 2015.

[3] J. Ni, L. Yao, J. Zhang, W. Cao, Y. Zhu and X. Tai, ”Development of an Unmanned Aerial Vehicle-Borne Crop-Growth Monitoring System,” Sensors, 2017.

[4] J. Bellvert, P. Zarco-Tejada, J. Girona and E. Fereres, ”Mapping crop water stress index in a Pinot-noir vineyard: comparing ground measurements with thermal remote sensing imagery from an unmanned aerial vehicle,” Precision Agriculture, vol. 15, no. 4, pp. 361-376, 2014.

[5] M. P. Christiansen, M. S. Laursen, R. N. Jrgensen, S. Skovsen and R. Gislum, ”Designing and Testing a UAV Mapping System for Agricultural Field Surveying,” Sensors, 2017.

[6] J. T. Snchez, F. L. Granados, N. Serrano, O. Arquero and J. M. Pea, ”High-Throughput 3-D Monitoring of Agricultural-Tree Plantations with Unmanned Aerial Vehicle (UAV) Technology,” PLOS: one, 24 June 2015.

[7] Y. Fang and R. P. Ramasamy, ”Current and Prospective Methods for Plant Disease Detection,” Biosensors, vol. 5, no. 3, pp. 537-561, September 2015.

[8] P. K. Sethy, B. Negi, S. K. Behera, N. K. Barpanda and A. K. Rath, ”An Image Processing Approach for Detection, Quantification, and Identification of Plant Leaf Diseases -A Review,” International Journal of Engineering and Technology (IJET), vol. 9, no. 2, April-May 2017.

[9] R. C. S. Nakano, A. Bandala, G. E. Faelden, J. M. Maningo and E. P. Dadios, ”Implementation of an artificial neural network in recognizing in-flight quadrotor images,” in 2015 IEEE Region 10 Conference TENCON, Macao, China, 2015.

[10] J. M. Z. Maningo, G. E. U. Faelden, R. C. S. Nakano, A. A. Bandala and E. P. Dadios, ”Obstacle avoidance for quadrotor swarm using artificial neural network self-organizing map,” in 2015 International Conference on Humanoid, Nanotechnology, Information Technology,Communication and Control, Environment and Management (HNICEM), Cebu City, Philippines, 2015.

[11] Y. Zeng, R. Zhang and T. J. Lim, ”Wireless communications with unmanned aerial vehicles: opportunities and challenges,” IEEE Communications Magazine, vol. 54, no. 5, pp. 36-42, 18 May 2016.

[12] D. Huang, D. Zhao and L. Zhao, ”A New Method of the Shortest Path Planning for Unmanned Aerial Vehicles,” in IEEE 6th Data Driven Control and Learning Systems Conference, Chongqing, China, 2017.

[13] S. Nuske, S. Choudhury, S. Jain, A. Chambers, L. Yoder, S. Scherer, L. Chamberlain, Cover, Hugh and S. Singh, ”Autonomous Exploration and Motion Planning for an Unmanned Aerial Vehicle Navigating Rivers,” Journal of Field Robotics, vol. 32, no. 8, pp. 1141-1162, 2015.

[14] C. YongBo, M. YueSong, Y. JianQiao, S. XiaoLong and X. Nuo, ”Three-dimensional unmanned aerial vehicle path planning using modified wolf pack search algorithm,” Neurocomputing, vol. 266, pp. 445-457, 2017.

[15] C. Di Franco and G. Buttazzo, ”Coverage Path Planning for UAVs Photogrammetry with Energy and Resolution Constraints,” Journal of Intelligent and Robotic Systems - Springer, 5 February 2016.

[16] C. Di Franco and G. Buttazzo, ”Energy-aware coverage path planning of UAVs,” in IEEE International Conference on Autonomous Robot Systems and Competitions, Italy, 2015.

[17] W. Zhan, W. Wang, N. Chen and C. Wang, ”Efficient UAV Path Planning with Multiconstraints in a 3D Large Battlefield Environment,” Mathematical Problems in Engineering, vol. 2014, p. 12, 2014.

[18] P. Sponagle and C. Salvaggio, ”Automatic mission planning algorithms for aerial collection of imaging-specific tasks,” SPIE, vol. 10218, pp. 1021807-1 to 1021807-13, 2017.

[19] N. H. Motlagh, T. Taleb and O. Arouk, ”Low-Altitude Unmanned Aerial Vehicles-Based Internet of Things Services: Comprehensive Survey and Future Perspectives,” IEEE Internet of Things Journal, vol. 3, no. 6, pp. 899-922, December 2016.

[20] P. Tokekar, J. V. Hook, D. Mulla and V. Isler, ”Sensor Planning for a Symbiotic UAV and UGV System for Precision Agriculture,” IEEE TRANSACTIONS ON ROBOTICS, vol. 32, no. 6, pp. 1498-1511, 2016.

[21] A. L. P. de Ocampo and E. P. Dadios, ”Energy cost optimization in irrigation system of smart farm by using genetic algorithm,” in 2017 IEEE 9th International Conference on Humanoid, Nanotechnology, Information Technology, Communication and Control, Environment and Management (HNICEM), Manila, Philiipines, 2017.

[22] R. L. Galvez, E. P. Dadios and A. A. Bandala, ”Path planning for quadrotor UAV using genetic algorithm,” in 2014 International Conference on Humanoid, Nanotechnology, Information Technology, Communication and Control, Environment and Management (HNICEM), Palawan, Philippines, 2014.